V International Conference on Particle-based Methods – Fundamentals and Applications
PARTICLES 2017
P. Wriggers, M. Bischoff, E. Oñate, D.R.J. Owen, & T. Zohdi (Eds)

GRAIN SCALE PARAMETERS IN DISSIPATIVE DRIVEN CONSTITUTIVE MODELS

RECTOR A. MUKWIRI[1], WILLIAM M. COOMBS[1], YOUSEF GHAFFARI MOTLAGH[2] AND CHARLES E. AUGARDE[1]

[1] School of Engineering and Computing Sciences
Durham University
Durham, DH1 3LE, UK
E-mail: r.a.mukwiri@durham.ac.uk, w.m.coombs@durham.ac.uk,
charles.augarde@durham.ac.uk
URL: https://www.dur.ac.uk/ecs/

[2] School of Chemical and Process Engineering
University of Leeds
Leeds LS2 9JT, UK
E-mail: Y.GhaffariMotlagh@leeds.ac.uk
URL: https://engineering.leeds.ac.uk/staff/859/Dr_Joseph_Ghaffari_Motlagh

Key words: DEM, energy dissipation, compression, sands, hyperplasticity

Abstract. Soil has generally been treated as a continuum from as early as the eighteenth century. Since then the analysis of soil behaviour in practical engineering analyses and development of constitutive models has depended on a continuum assumption. However, in order to gain a deeper understanding of the behaviour of soils and their particulate nature, there is a need to move from continuum mechanics to discrete models. Such modelling is possible using the Discrete Element Method (DEM). In this paper an open source DEM particle simulation software, LIGGGHTS is used to study the relationships between grain scale parameters and energy dissipation in granular media in one-dimensional compression. The influence of particle size distribution, void ratio, and inter-particle friction coefficient on energy dissipation are studied and discussed. In order to measure the dissipated energy, changes in energy terms are traced at every time step and the principle of energy conservation applied. It is hoped that the knowledge gained of the relationship between grain scale parameters and energy dissipation will help in the formulation of constitutive relationships within the hyperplasticity framework. It is envisioned that relating grain scale parameters to constitutive models will allow the formulation of models that are purely based on the micro-mechanics of granular media.

1 INTRODUCTION

Soil has generally been treated as a continuum from as early as the eighteenth century [2]. This assumption has since then been used in engineering design for practical purposes. Indeed many constitutive models are built on this assumption. However, in order to understand soils better, we need to move from continuum mechanics to a discrete method of study. Such a method is the Discrete Element Method (DEM) originally introduced by Cundall and Strack [1]. The DEM allows us to study soil at a particle level and gain a better understanding of its behaviour. Studying soil at grain scale will hopefully minimise the need to make assumptions when defining constitutive models. The DEM is here used to investigate grain scale parameters in relation to energy dissipation, a core component of the hyperplasticity approach to constitutive modelling [6].

The hyperplasticity approach allows the constitutive behaviour of a material to be derived from a free-energy function and a dissipation rate function [6]. This approach stems from the works of Ziegler[12] and Houlsby [5]. Once these scalar functions have been specified, the yield function, flow rule and the stress and strain relationships can be derived without need of any additional assumptions. The first scalar function is derived from the First law of Thermodynamics and the dissipation function is a consequence of the Second law of Thermodynamics.

By understanding the fundamental causes of energy dissipation in a DEM simulation, a dissipation function could potentially be formulated leading to a constitutive relationship formulation directly informed by physical measurements at a particle level. In this paper, relationships between energy dissipation and grain scale parameters for one-dimension compression problems are discussed. The grain scale parameters explored are: the inter-particle friction coefficient, particle size distribution and the initial void ratio. The relationship between these parameters and energy dissipation is discussed.

The rest of the paper is laid out as follows. Section 2 will describe the simulation procedure followed for the DEM simulations. In Section 3 the energy calculations are detailed. Section 4 describes parameters varied in this paper. The results from the simulations are reported and described in Section 5. The paper will finally provide some conclusions in Section 6.

2 SIMULATION PROCEDURE

One-dimensional compression simulations were carried out using DEM. An open source DEM particle simulation software, LIGGGHTS, developed by Kloss et al. [7] was used for this study. Unlike commercial DEM software, LIGGGHTS has no user interface. A simulation is driven using a text-based input script containing a series of commands to conduct the simulation. This input script is read sequentially making the ordering of statements important. Before the execution commands, the input script should have the initialisation settings specified and the simulation set up.

The initialisation settings and parameters are those that need to be specified before

the particles can be generated. These settings and parameters include the boundary style, units, region size, neighbour sorting, time step size, and atom style. In this study the boundary was specified to be of a moving style to allow vertical movements during loading and unloading.

To ensure a stable simulation, a time step, Δt of 1×10^{-7}s was used. When a very large time step is used, some of the contacts are not detected since the acceleration values that used to update the particle positions are not current. This value was arrived at based on the method for calculating the DEM critical time step proposed by O'Sullivan and Bray [11] for different particle arrangements. For non uniform contacts arrangement, the critical time step is given as $0.221\sqrt{m/K}$ where m is the particle mass and K is the contact stiffness was taken to be the greater of either the normal or tangential contact stiffness values. For a stable simulation, a value equal to or less than the critical value needs to be used.

The simulated particles where spheres of Poisson's ratio of 0.25, Young's modulus of 70MPa, and density of 2650kg/m^3 per particle. The density value was chosen based on the fact the dominant mineral in sands is quartz, which has a density of 2650kg/m^3. This value is also typically adopted in the DEM simulation of sands (for example in [3] and [9]).The particle-wall coefficient of friction was kept at zero.

After all the specific settings and parameters were specified, a model of a cylinder with a covered base extending to the simulation bounds, and a top circular mesh to cover the sample were input to the simulation as STereoLithography (STL) files to provide an enclosure of 30mm diameter by 10mm height. These meshes were made of triangular elements. Particles were then packed in the enclosed space and then allowed to settle.

The particles were then densified to different initial void ratio values in the range 0.43 - 0.7 by moving the top platen downwards at constant velocity, following which the particles were allowed to settle. The void ratio is calculated as

$$e = \frac{V_v}{V_s}, \tag{1}$$

where V_v and V_s are volumes of void and solids respectively. The top platen vertical velocity was calculated from

$$v_{mesh} = \frac{V_s(e_{tar} - e_{cv})}{t_{steps}\pi R^2 \Delta t}, \tag{2}$$

where e_{tar} and e_{cv} are the target and current void ratios, t_{steps} is the number of time steps to run, and R is the sample radius. After being densified, the particles were then compressed to $e_{tar} = 0.2$ on the loading cycle then unloaded to their initial void ratio value. Figure1 shows a sketch of the simulations before (a) and at the end of loading (b), and at the end of unloading (c). At the end of unloading, the samples had undergone some permanent deformation compared to the start of the simulation due to the rearrangement of particles.

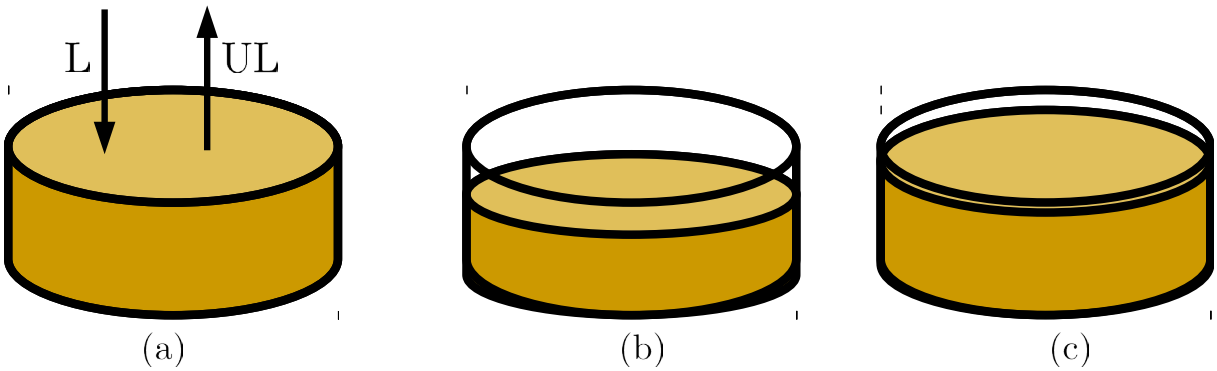

Figure 1: Loading (L) and unloading (UL): (a) before loading samples; (b) end of loading; (c) end of unloading

Results files were output throughout the simulation for later post processing for energy calculations. The particle data output included: position vectors, velocity values, total forces, particle radii and IDs, normal and tangential contact forces, and particle-particle overlap distances. These data were output every 25000 time steps, which was found to be sufficient data to understand the various behaviours during simulations. The stress data on the meshes was also output at the same intervals in separate files and later post processed to give the compression force.

3 ENERGY MONITORING

To facilitate the study of energy dissipation for the tests conducted, energy monitoring was done by post processing the files output during the simulations using Matlab. The energy equation used was

$$dE_p + dW = dE_k + dE_\mu + dE_\zeta + dU, \tag{3}$$

where dE_p is the change in potential energy, dW the change in boundary work, dE_k the change in kinetic energy, dE_μ the dissipated frictional energy, dE_ζ the change in dissipated energy through damping, and dU the change in stored work.

The total change in dissipated energy, dE_η during the simulations comes from the dE_μ and dE_ζ terms of (3). Since the simulations are pseudo-static, it was found that the potential and kinetic energies were usually each $\approx 10^6$ times smaller than either of the boundary work or the stored elastic energy. We can therefore re-write (3) as

$$dE_\eta \approxeq dW - dU \tag{4}$$

The change in boundary work is calculated as:

$$dW = \left(\sum_{j=1}^{m} \sigma_v^j A_S^j \right) \delta x, \tag{5}$$

where σ_v^j is the normal stress on mesh j, m is the total number of mesh elements on the boundary mesh considered, and δx is the change in displacement of the boundary mesh. A_S^j is the surface area of triangular mesh element j considered and is obtained by

$$A_S^j = \frac{1}{2}|\mathbf{AB} \times \mathbf{AC}|, \tag{6}$$

where the area of each triangular element with vertices A, B and C is calculated from the cross product between vectors **AB** and **AC**.

Changes in the stored energy are due to the evolution of normal and tangential contact forces. The summation of strain energy for all the contacts is equal to the stored energy, dU and is calculated as

$$dU = dU^n + dU^t, \tag{7}$$

where dU^n and dU^t are the contributions from normal and tangential contact forces and are equal to

$$dU^n = \int_0^{\delta_n} \underbrace{\overbrace{\frac{4}{3}E^*\sqrt{R^*\delta_n}}^{K_n}\,\delta_n \mathbf{n}}_{F^n}\, d_n \tag{8}$$

and

$$dU^t = \int_0^{\xi_t} \underbrace{\overbrace{8G^*\sqrt{R^*\delta_n}}^{K_t}\,\boldsymbol{\xi_t}}_{F^t}\, d\xi_t, \tag{9}$$

respectively. F^n and F^t are in turn the normal and tangential contact forces and K_n and K_t are the corresponding stiffness parameters from the Hertzian contact model, which governed how the spherical particles interacted at contact. Two particles 1 and 2 have an effective radius, $R^* = R_1R_2/(R_1 + R_2)$, which is the geometric mean of radii R_1 and R_2. $\delta_n = R_1 + R_2 - d_{12}$ and is the overlap at contact between the two particles in the normal direction where d_{12} is the distance between their centres. The effective Young's modulus, $E^* = 0.5E/(1 - \nu^2)$, is derived from the particles' material Young's modulus, E and Poisson's ratio, ν. In Equation (8), $\mathbf{n}$ is the normal vector for the particles in contact. The term $\boldsymbol{\xi_t}$ in Equation (9) is the tangential displacement and is calculated by integrating the tangential relative velocity over the contact time [4].

4 SIMULATION PARAMETERS VARIED

Sands are typically made up of different grain sizes which give rise to Particle Size Distributions (PSDs). These can be defined using the coefficient of uniformity (C_u), which is a shape parameter given as

$$C_u = \frac{d_{60}}{d_{10}}. \tag{10}$$

d_{60} and d_{10} respectively are particle diameters for which 60% and 10% of the material by mass is finer. PSDs affect the soil responses. For example, McDowell and Bolton [8] studied the effect of particle size distribution on pile end resistance using two PSDs. It was found that the peak pile resistance during penetration was a function of the PSD. Smaller particles increased the level of resistance in the soil. PSD also affects the compressibility of grains [9].

Friction between particles, μ is means by which most energy is dissipated in granular media. The friction coefficient between particles was therefore varied along with PSD and the initial void ratio, e_{ini} in the present study with no particle crushing involved. Table 1 shows the varied parameters for each simulation. Results from these simulations are discussed next.

Table 1: Simulation test parameters

Simulation	C_u	e_{ini}	μ
1	1	0.7	0.5
2	1.3	0.7	0.5
3	2	0.7	0.5
4	2	0.7	0.2
5	2	0.7	0.25
6	2	0.7	0.3
7	2	0.7	0.35
8	2	0.7	0.4
9	2	0.7	0.45
10	2	0.7	0.5
11	2	0.67	0.5
12	2	0.64	0.5
13	2	0.61	0.5
14	2	0.58	0.5
15	2	0.55	0.5
16	2	0.52	0.5
17	2	0.49	0.5
18	2	0.46	0.5
19	2	0.43	0.5

5 RESULTS AND DISCUSSION

Minh and Cheng [10] observed that the compression of sands is due to the rearrangement of particles and elastic compression. During unloading of the sand sample, particles would be unstressed but would not have the same level of rearrangement as in the loading, and would have experienced unrecoverable deformation. These observations should be reflected in the energy dissipation curves for simulations.

The results from the current study show that a higher C_u results in less energy dissipation for $1 < C_u \leq 2$ as shown in Figure 3 for simulations 1-3 in Table 1. This observation may be explained as follows. As smaller particles are introduced, the particle contacts network becomes more resistant to sliding. More of the input energy is as a result stored. This suggests that the rate of energy dissipation for these simulations is negatively correlated to the coefficient of uniformity.

Figure 2 shows a plot of the void ratio against the vertical stress for simulations 1-3 in Table 1. The circled part highlights an area where the pressure drops. There is a sudden rearrangement within the specimen of $C_u = 1$ and $C_u = 1.3$ due to pockets of voids being filled rapidly. This change in pressure results in an increase of dissipated energy corresponding to the rearrangement of particles.

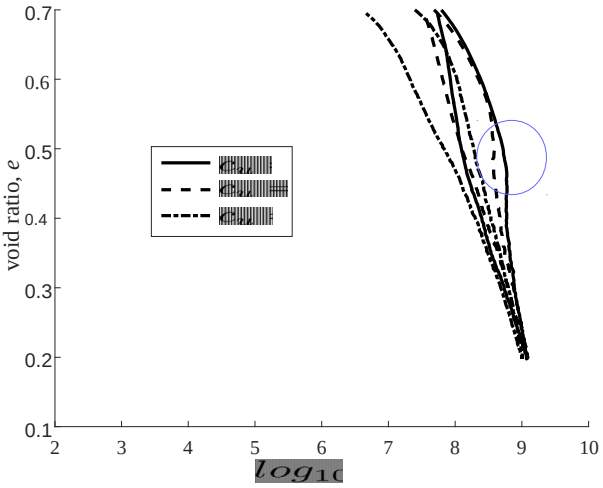

Figure 2: e-logσ_v

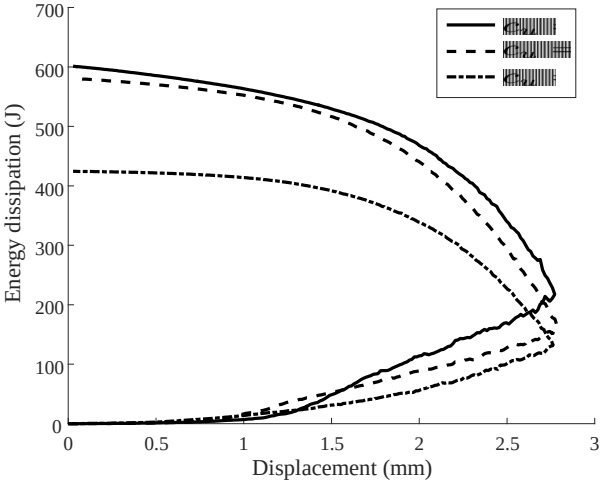

Figure 3: Dissipated energy against displacement

The inter-particle friction coefficient (μ) was varied between 0.5 and 0.2. The friction coefficient affects how fast the particles can be packed, a feature observed during the insertion of particles. A lower friction coefficient makes it easier to pack particles. Though not utilised in this paper, this fact is generally exploited to speed up the particle packing stage of the simulation by using a low μ value during the particle insertion stage and changing it to the desired value later.

Figure 4 shows a plot of void ratio against the log of vertical stress graphs for the different μ values. The variation between different μ values is not significant. This is mainly due to the fact that changes in void ratio are largely due to the compression of the particles which is mainly governed by the movement of the top platen.

A higher friction coefficient results in more energy dissipation during loading as observed in Figure 5 for Simulations 4-9 (Table 1). This is consistent with the fact that energy is largely lost through friction. Less energy is dissipated on the unloading curves because of some permanent settlement of particles during compression, however the trend of energy dissipation is still directly proportional to the friction coefficient. The rate of energy dissipation based on this result would therefore be expected to be positively correlated with the inter-particle coefficient of friction.

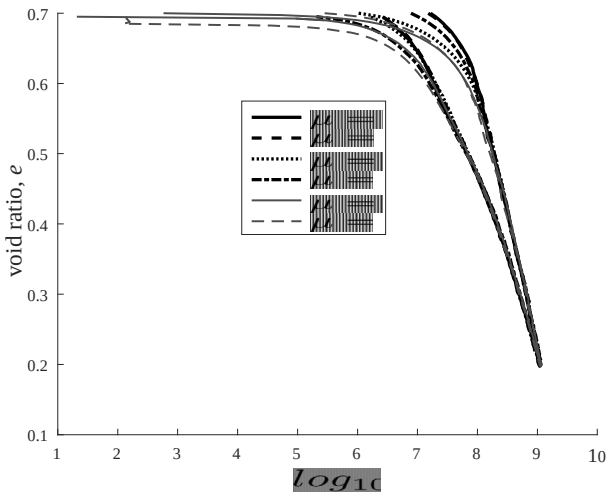

Figure 4: e-logσ_v

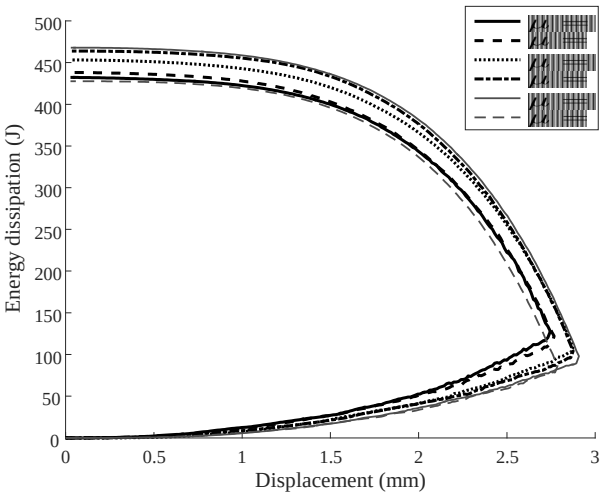

Figure 5: Dissipated energy against displacement

Loading and unloading cycles were simulated for ten different initial void ratios (e_{ini}) from $0.7-0.43$ (see Table 1: simulations 10-19). Results from these simulations are shown in Figure 6. It can be seen from this graph that towards the end of simulations a similar compression path was followed as would be expected. The differences correspond to the oscillations of particles during the simulations.

The energy dissipation curves shown in Figure 7 become steeper with a decreasing e_{ini} during compression. This is because more input work is required to move particles through the same displacement and since most of this work is not stored energy, then it is dissipated largely through friction. It can also be seen that there is a similar steepness achieved at a greater displacement for samples with a higher e_{ini}. On unloading, more energy is dissipated as the e_{ini} decreases. These results suggest that the rate of energy dissipation is negatively correlated with the initial void ratio.

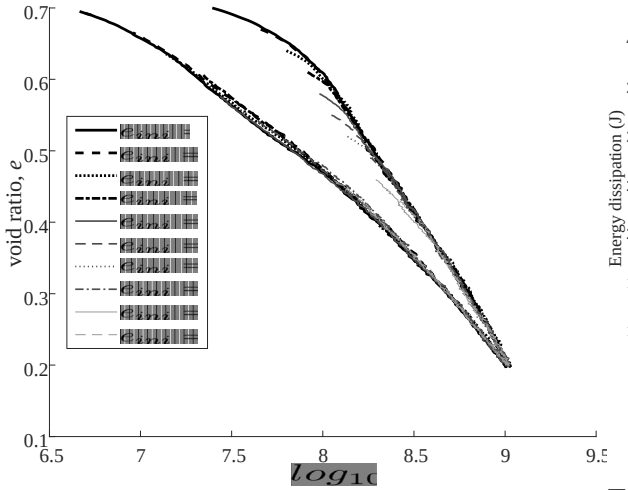

Figure 6: e-logσ_v

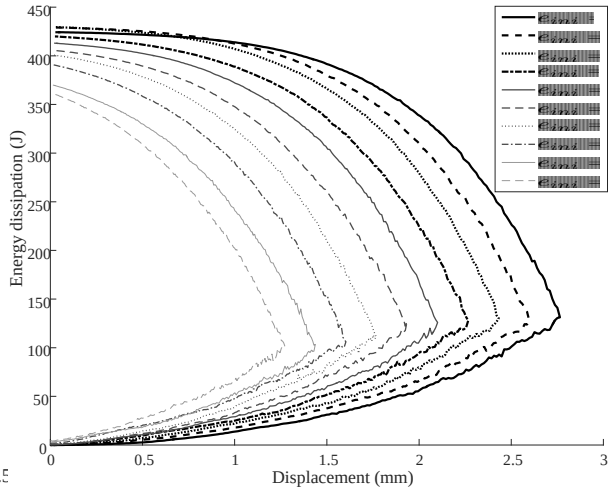

Figure 7: Dissipated energy against displacement

6 CONCLUSIONS

One-dimensional compression tests using the DEM have been conducted including loading and unloading cycles using spherical particles whose properties were set to those of sands. Throughout these simulations, data was output and then post processed in Matlab for energy dissipation. PSD, initial void ratio, and the coefficient of friction were the three parameters varied in the present study. Increasing the coefficient of uniformity was found to decrease the energy dissipated. It was proposed that this observation is due to the fact that as smaller particles are introduced, which reduce on the sliding of particles while increasing the amount of stored energy. A lower initial void ratio resulted in steeper curves for energy dissipation and is due to the fact that more input energy is required to move the particles through the same displacement at lower e_{ini} values most of which is dissipated. A higher friction coefficient between particles resulted in more energy dissipation during loading and unloading of the samples. This is due to the fact that energy is mainly lost through friction, which is directly proportional to its coefficient. A negative correlation between energy dissipation rates for the simulations conducted with either e_{ini} or C_u is envisioned. On the other hand, a positive correlation between the inter-particle coefficient of friction with the energy dissipation rate is expected. It is hoped that studies of the relationship between grain scale parameters and energy dissipation will lead to the formulation of the constitutive models directly informed by grain scale parameters.

REFERENCES

[1] P. A. Cundall and O. D. L. Strack. A discrete numerical model for granular assemblies. *Géotechnique*, 29:47–65, 1979.

[2] R. Davis and A. Selvadurai. *Plasticity and Geomechanics*. Cambridge University Press, 2002.

[3] J. P. De Bono and G. R. McDowell. Discrete element modelling of one-dimensional compression of cemented sand. *Granular Matter*, 16:79–90, 2014.

[4] X. Dou, Y. Mao, and Y. Zhang. Effects of contact force model and size distribution on microsized granular packing. *J. Manuf. Sci. Eng*, 136(2):021003, 2014.

[5] G. Houlsby. *A Study of Plasticity Theories and Their Applicability to Soils*. PhD thesis, University of Cambridge, 1981.

[6] G. Houlsby and A. Puzrin. *Principles of Hyperplasticity*. Springer, 2006.

[7] C. Kloss, C. Goniva, A. Hager, S. Amberger, and S. Pirker. Models, algorithms and validation for opensource DEM and CFD-DEM. *Progress in Computational Fluid Dynamics, An Int. J.*, 12:140–152, 2012.

[8] G. McDowell and M. Bolton. Effect of particle size distribution on pile tip resistance in calcareous sand in the geotechnical centrifuge. *Granular Matter*, 2:179–187, 2000.

[9] G. McDowell and J. de Bono. On the micro mechanics of one-dimensional normal compression. *Géotechnique*, 3:166–172, 2013.

[10] N. H. Minh and Y. P. Cheng. A dem investigation of the effect of particle-size distribution on one-dimensional compression. *Géotechnique*, 63:44–53, 2013.

[11] C. O'Sullivan and J. Bray. Selecting a suitable time-step for discrete element simulations that use the central difference time integration approach. *Engineering Computations*, 21(2-4):278–303, 2003.

[12] H. Ziegler. *An introduction to thermomechanics*. North Holland Pub. Co, Amsterdam, 2nd edition, 1983.